Received 24 November 2025
Revised 21 January 2026
Accepted 23 January 2026

Study on fatigue property of the rib-to-deck welded joint in orthotropic steel bridge deck, considering the weld penetration rate

Xiaochen Ju and Zhibin Zeng
Bridge Department,
China Academy of Railway Sciences Corporation Limited Railway Engineering Research Institute, Beijing, China, and
Shen Rao
School of Mechanical and Electronic Control Engineering, Beijing Jiaotong University, Beijing, China

Abstract

Purpose – The U-shaped rib-to-deck welded joint in orthotropic steel decks (OSDs) is prone to multiple fatigue cracks, which threaten structural integrity. Current design codes worldwide stipulate a minimum weld penetration rate of 75% or 80%, but practical challenges exist in meeting these requirements due to welding process limitations and machining errors. This study aims to investigate the influence of weld penetration rate on the fatigue performance of such joints, providing a theoretical basis for optimizing design and construction schemes.

Design/methodology/approach – Firstly, finite element models of U-shaped rib-to-deck welded joints with penetration rates of 65%, 75%, 85% and double-sided welds were established to analyze mechanical characteristics under typical loading conditions. Fatigue tests were then conducted on specimens with different penetration rates, and phased array ultrasonic testing technology was employed to assess penetration depth. Finally, fatigue S-N curves were regressed for partial penetration and double-side welded joints to quantify fatigue performance.

Findings – Stress concentration at the weld root decreases with the increase of penetration rate in partial penetration welds, while double-sided welds eliminate the weld root and further reduce stress concentration. Penetration depth exhibits significant dispersion even within the same weld. Partial penetration welds mainly initiate cracks from the weld root and propagate along the weld throat, whereas double-sided welds initiate cracks from the inner weld toe and propagate along the rib web. The fatigue strength of double-sided welds (143.9 MPa) is significantly superior to that of partial penetration welds (96.9 MPa) at 2×106 cycles.

Originality/value – This study fills the gap of limited experimental data on the fatigue performance difference between partial penetration and double-side rib-to-deck welded joints. The findings clarify the influence mechanism of penetration rate on fatigue behavior, providing valuable theoretical support and technical reference for the design optimization, construction quality control and maintenance decision-making of OSD welded joints.

Keywords Fatigue property, Weld penetration rate, Rib-to-deck welded joint, Orthotropic bridge deck

Paper type Research article

1. Introduction

Orthotropic steel deck (OSD) has emerged as a prevalent choice for the bridge deck structure in large and medium-span steel bridges globally, celebrated for its lightweight construction, high ultimate bearing capacity, and rapid construction period. However, the occurrence of

Funding: This work was supported by China Academy of Railway Sciences (award no. 2024YJ204).

fatigue cracks has been observed in some bridges soon after entering service, presenting a significant challenge to the structural integrity of OSDs.

Three distinct types of fatigue cracks commonly manifest in OSDs: those adjacent to the rib-to-deck welded joints, near the cross weld between U-shaped ribs and diaphragm plates, and at the butt weld between U-shaped ribs. Notably, the U-shaped rib-to-deck welded joint bears the combined effect of local tension (or compression) and bending induced by wheel loads perpendicular to the deck plate. According to incomplete statistics, fatigue cracks near the rib-to-deck welded joints contribute to approximately 30.2% of the total fatigue cracks observed in OSDs in China. Therefore, considering the pivotal role these joints play in the overall structural integrity of OSDs, it is crucial to address this issue.

Currently, the predominant welding method for U-shaped rib-to-deck joints is a partial penetration weld. Various international design codes, including China's "Code for Design of Highway Steel Structure Bridges" (JTG D64-2015) (Ministry of Transport of the People's Republic of China, 2015), "Code for Design of Railway Bridge Steel Structures" (TB 10091–2017) (National Railway Administration of the People's Republic of China, 2017), Japan's "Fatigue Design Guidelines for Steel Highway Bridges" (2002), the American "AASHTO LRFD Bridge Design Specifications" (2012), and Eurocode 3 "Design of Steel Structures" (2005), stipulate penetration depth or rate requirements to ensure the structural reliability of these welds.

Several studies have extensively explored the fatigue resistance of U-shaped rib-to-deck welded joints in OSDs. Xiao, Yamada, Ya, and Zhao (2008) and Wang, Fu, Wei, and Wang (2023) conducted stress analyses and fatigue evaluations, revealing that an increase in the distribution area of wheel load or deck plate thickness can reduce the stress range on the deck plate and significantly enhance the fatigue life of rib-to-deck welded joints. Cui, Zhang, Luo, Hao, and Li (2018) focused on estimating the fatigue reliability of these joints by considering the combined effects of welding residual stress and stochastic traffic flow. Sim, Uang, and Sikorsky (2009), Sim and Uang (2012), and Chen, Wei, and Zhao (2023) studied the impact of weld double-side and distortion control measures on fatigue resistance. Ya, Yamada, and Ishikawa (2011) conducted fatigue tests on rib-to-deck specimens with 3 weld details (80% partial penetration weld, double-sided weld, and the combination of the two), revealing slightly lower fatigue strengths in specimens with double-sided welds compared to 80% partial penetration welds. Pu, Gao, Liu, and Shi (2013) and Cui, Bu, and Zhang (2015) introduced the structural hot spot approach for calculating fatigue resistance. However, these studies focused primarily on theoretical investigations without direct verification through actual measurements. Wei and Jiang (2017) and Ju and Tateishi (2014) evaluated fatigue life based on fracture mechanics, while Tao (2013), Tong, Wang, Yu, Zhao, and Xu (2023), and Wang, Dong, Pan, and Ma (2020) conducted fatigue tests using full-scale orthotropic deck specimens based on different engineering parameters, obtaining valuable mechanical data near rib-to-deck welded joints in OSDs. Chen *et al.* (2024) developed a fracture-mechanics-based fatigue reliability model for OSD welded joints under vehicle loads and residual welding stresses. Li *et al.* (2024) highlighted how weld penetration and geometry influence fatigue performance. Li *et al.* (2023) discussed effects such as repair welding on fatigue crack propagation and life prediction for orthotropic rib-to-deck welded joints. Until now, the experimental data on the fatigue property between partial penetration and double-side rib-to-deck welded joint are limited.

In this study, the influence of penetration rate, which is the ratio of penetration depth of the U-shaped rib to its thickness, on the fatigue performance of U-shaped rib-to-deck welded joints was investigated through both finite element analysis and experimental testing to find the actual difference in fatigue property between partial penetration and double-side rib-to-deck welded joints.

2. Finite element analysis

2.1 Model information

To conduct a detailed analysis, the large-scale general finite element analysis software ABAQUS was employed to establish a refined finite element model of an orthotropic steel bridge deck segment. The model, as depicted in Figure 1, incorporates an elastic modulus of 2.1 × 10^5 MPa and a Poisson's ratio of 0.3. The element type utilized is an 8-node three-dimensional solid element.

The model comprises 6 U-shaped ribs and 4 diaphragms with a spacing of 3,200 mm. Specific dimensions include a 16 mm thickness for the bridge deck, 8 mm for the U-shaped ribs, and 10 mm for the diaphragms. The U-shaped ribs are spaced at intervals of 600 mm.

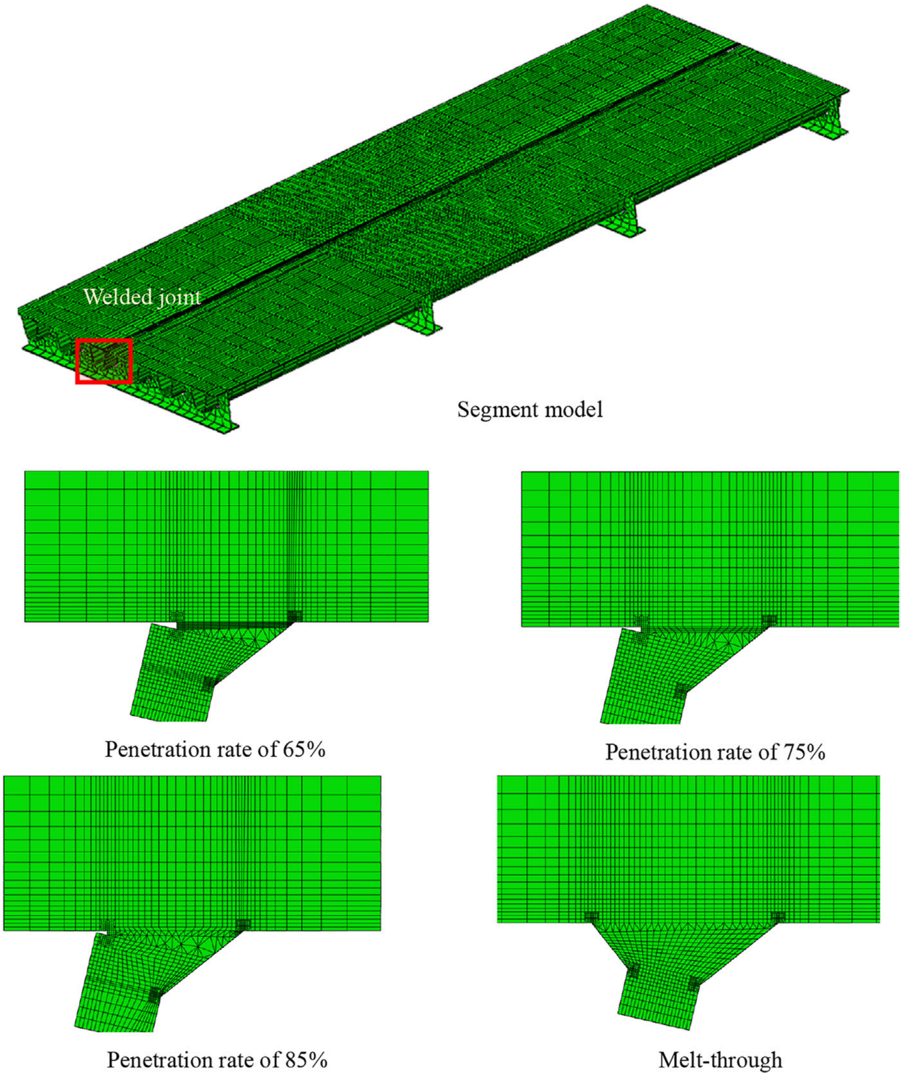

Figure 1. Finite element model. **Source(s):** Authors' own work

A contrast analysis of Von Mises stress was conducted for U-shaped rib-to-deck welded joints, considering weld penetration ratios of 65%, 75%, 85%, and double-sided welds. To mitigate the influence of element size on calculation accuracy, the element size at stress concentration points of the joints was meticulously controlled to approximately 0.2 mm.

2.2 Loading information

The analysis adopted a rear axle single-wheel load of 70 kN, following the guidelines outlined in China's "General Specification for Highway Bridge and Culvert Design" (JTG D60-2015). The defined contact area between the wheel and the bridge deck measures 600 mm × 200 mm.

In the transverse direction, 3 representative loading positions were selected, as illustrated in Figure 2. Position 1 is directly above the midpoint between two U-shaped ribs. Position 2 is directly above the single-sided web of one U-shaped rib. Position 3 is directly above the center of one U-shaped rib.

Moving along the longitudinal direction, nine load positions were strategically chosen at intervals of 200 mm, extending from one transverse diaphragm to the mid-span position of two transverse diaphragms. Consequently, the analysis model encompassed a total of 27 loading positions, ensuring a comprehensive assessment of the structural response.

2.3 Analysis results discussion

Four types of potential fatigue cracks near U-shaped rib-to-plate welded joints in OSDs are illustrated in Figure 3. Among them, Crack 1 and Crack 3 are the most common, originating from the welding root. Crack 2 and Crack 4, originating from the welding toe, have also been observed in real bridges. This study primarily focuses on the stress at the initial points of these 4 cracks. The corresponding points in the finite element model are denoted as P1, P2, P3, and P4, as illustrated in Figure 4.

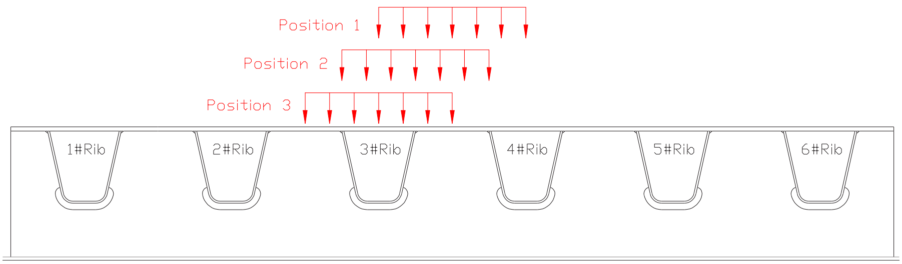

Figure 2. Transverse loading positions. **Source(s):** Authors' own work

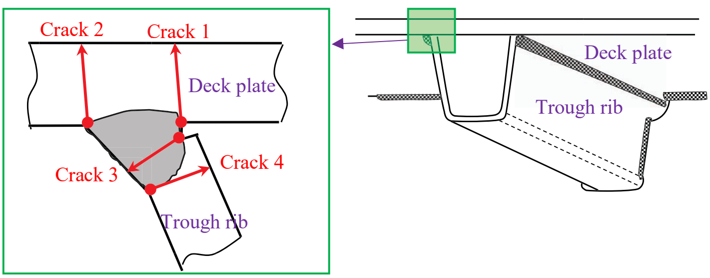

Figure 3. Typical fatigue cracks at rib-to-plate welded joints. **Source(s):** Authors' own work

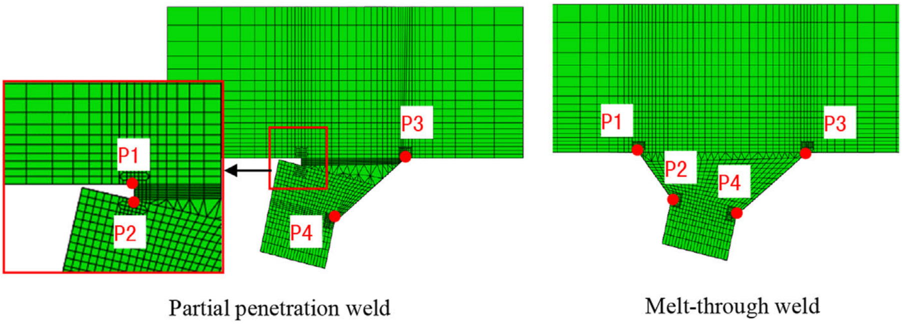

Figure 4. Focused points. **Source(s):** Authors' own work

Table 1 presents the peak values of Von Mises stress at the mid-span position for 4 welded joints with different penetration rates. Under Loading Position 1, the stress concentration at points P1 and P2 is more pronounced. For Loading Positions 2 and 3, the stress at points P1 and P3 is larger than that at other points. Among the 3 different transverse loading positions, the stress concentration at point P1 is the most evident. The stress at point P1 significantly decreases as the penetration rate increases. This reduction implies a lower probability of fatigue cracking. As the penetration rate increases, the notch between the U-shaped rib and plate becomes smaller; therefore, the stress at the P1 and P2 decreases. However, the stress at the P3 and P4 increases.

Furthermore, an analysis was conducted to examine the influence of changes in loading position in the longitudinal direction on the stress state, as illustrated in Figure 5. As the wheel load moves from one diaphragm to the mid-span position of two diaphragms, the stress at the 4 investigated points increases linearly. However, a sudden increase in stress occurs when the wheel load is positioned directly above the 4 investigated points at the mid-span position.

3. Fatigue test

3.1 Welding parameters

In this study, the welding methods employed include a single-side fillet weld for partial penetration welds and a double-side submerged arc welding process for double-sided welds. The partial penetration welds, utilizing a conventional ship position weld with two pass welds, involve the synchronous welding of internal fillet welds on both sides of multiple U-shaped ribs on a flat scaffold. Subsequently, external welds are formed simultaneously on an oblique scaffold. Both internal and external welds are completed in a single pass. The specific welding parameters are detailed in Table 2.

Table 1. Von Mises stress peak values under different loading positions (MPa)

Penetration rate	Position 1				Position 2				Position 3			
	P1	P2	P3	P4	P1	P2	P3	P4	P1	P2	P3	P4
65%	90.2	69.7	45.8	9.7	93.9	51.6	67.2	32.4	79.3	30.8	71.3	56.0
75%	83.9	66.1	44.3	8.7	90.6	50.9	72.5	34.8	71.7	29.7	73.0	59.1
85%	80.1	55.2	43.4	7.8	85.9	41.5	71.8	34.6	67.7	23.8	72.8	60.9
Double-side	59.1	59.2	56.9	14.2	74.1	40.4	80.2	39.7	68.9	15.6	82.1	59.6

Source(s): Authors' own work

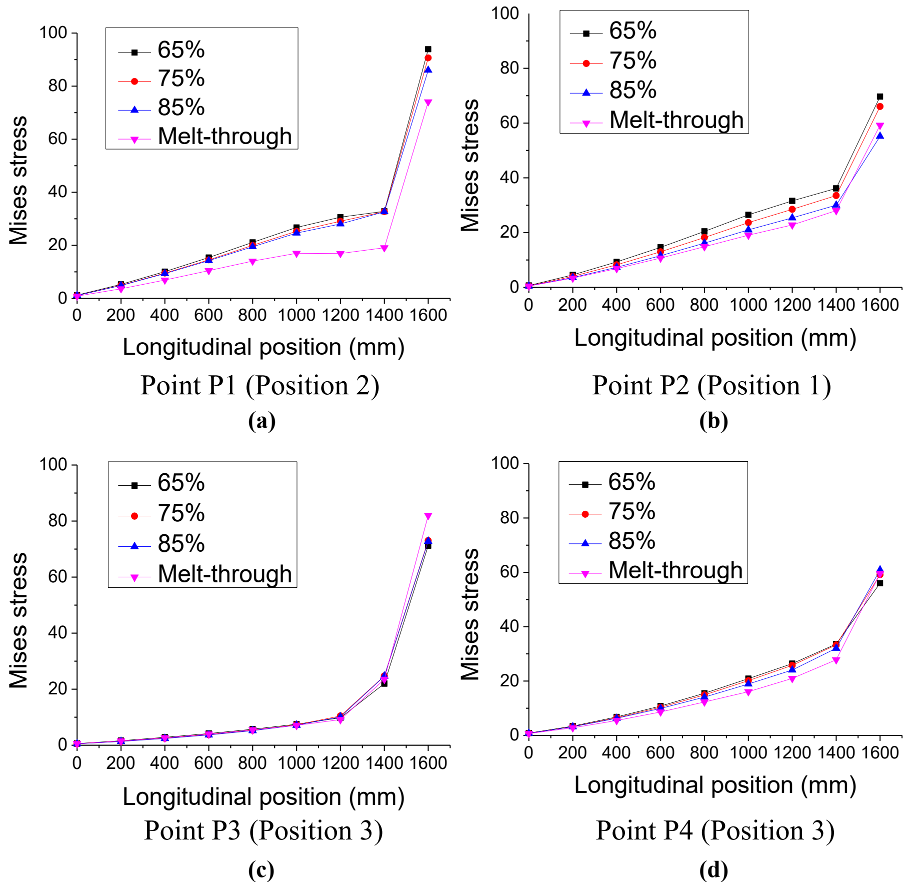

Figure 5. Stress change due to loading position change. **Source(s):** Authors' own work

When employing partial penetration welds in rib-to-deck joints, achieving a correspondence between the actual weld penetration rate and the design penetration rate proves challenging, as illustrated in Figure 6. Notably, even within the same pass weld, variations in penetration rate are observed across different sections, as depicted in Figure 7.

To quantify these variations, the weld penetration rate of two-pass welds (A and B) in rib-to-deck joints for 18 test specimens was assessed using phased array ultrasonic detecting technology. The specimens, each with a length of 300 mm, were divided into 3 sections (Line1, Line2, Line3), spaced 100 mm apart along the length direction, as shown in Figure 6. The weld penetration rate test results are tabulated in Table 3, revealing significant disparities in the penetration rate, even within the same pass weld.

The average values of actual penetration rates for design penetration rates of 65%, 75%, and 85% are 72.2%, 77.6%, and 85.9%, respectively. It can be found that the shape of the weld was difficult to keep uniform for the different penetration rates, which may be a factor affecting fatigue performance. Concurrently, the frequency distribution of the measured penetration rate is analyzed. Notably, the frequency for design penetration rates of 65% and 85% exhibits greater dispersion, resembling a skewed distribution. Conversely, the frequency for the design penetration rate of 75% generally conforms to a normal distribution.

Table 2. Welding parameters

Design penetration rate	65%		75%		85%		Double-side	
Root face (mm)	3.5		2.5		1.5		4	
Bevel angle (°)	50		50		50		55	
Welding pass	No.1	No.2	No.1	No.2	No.1	No.2	Inner	Outer
Welding method	Ar-rich gas shielded welding	CO_2 gas shielded welding	Ar-rich gas shielded welding	CO_2 gas shieled welding	Ar-rich gas shielded welding	CO_2 gas shieled welding	Submerged arc welding	Submerged arc welding
Type of welding wire	ER50-6	E501T-1	ER50-6	E501T-1	ER50-6	E501T-1	MCJQ-3	MCJQ-3
Diameter of welding wire (mm)	1.2	1.2	1.2	1.2	1.2	1.2	1.6	3.2
Gas composition	80%Ar+ 20% CO_2	/	80%Ar+ 20% CO_2	/	80%Ar+ 20% CO_2	/	/	/
Welding current (A)	350	260	320	240	340	260	380	570
Welding voltage (V)	32	28	31	26	31	28	31	31
Gas flow (*l*/min)	25	25	25	25	25	25	/	/
Welding speed (mm/min)	400	380	400	320	450	360	450	550

Source(s): Authors' own work

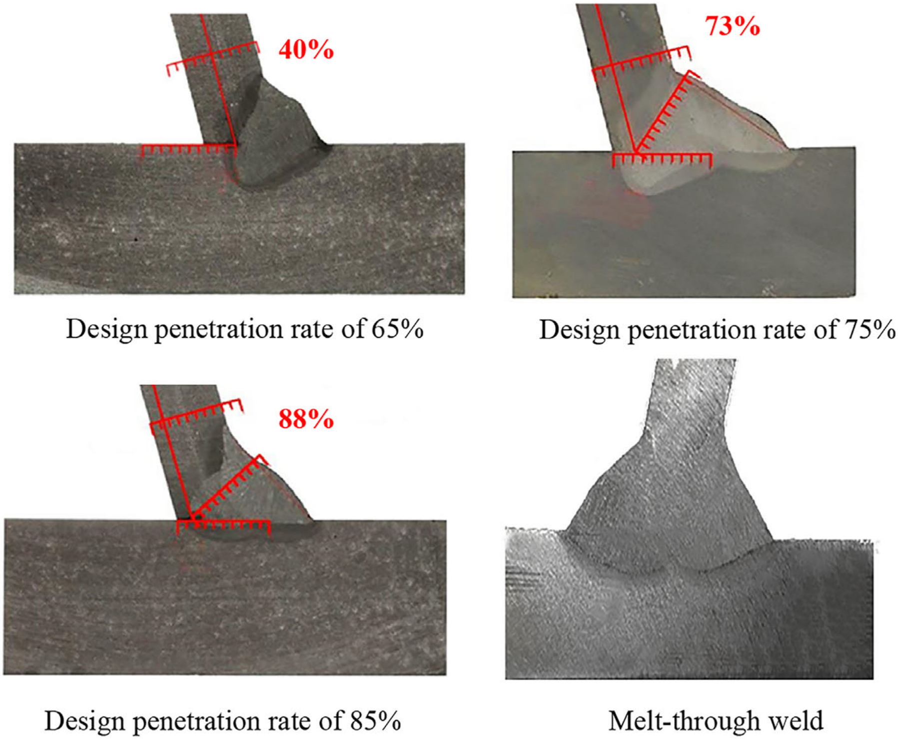

Figure 6. Appearance of rib-to-deck welded joint. **Source(s):** Authors' own work

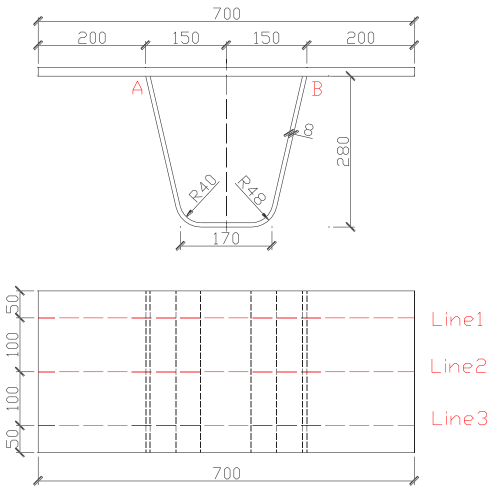

Figure 7. Detected sections of the penetration rate test. **Source(s):** Authors' own work

Table 3. Penetration rate of rib-to-plate welding joints (%)

Design penetration rate	Average actual penetration rate (%)	Standard deviation	Penetration rate range of tested sections (%)
65	72.2	15.0	26.3–100.0
75	77.6	9.4	57.5–100.0
85	85.9	10.1	58.8–100.0

Source(s): Authors' own work

3.2 Test overview

In the case of partial penetration welding, fatigue cracks predominantly initiate from the welding root. When the wheel load acts on the area between adjacent U-shaped ribs, both the plate and the U-shaped rib are subjected to tension (or pressure) and bending moment simultaneously, resulting in a tensile stress concentration state at the welding root–this represents a particularly unfavorable loading scenario.

To address this, fatigue specimens and a loading device were designed, as illustrated in Figures 6 and 8. The fatigue specimen, mimicking the size of actual OSDs, is a single U-shaped rib specimen with a width of 700 mm and a length of 300 mm. The test load is applied to the two sides of the deck plate, while the lower part of the U-shaped rib is securely fixed to the foundation support using bolts. The finite element model of the test specimen and a real bridge segment were established to verify the consistency of the force state. The force state near the rib-to-plate welded joint in the actual bridge and the test specimen remains essentially consistent.

During the fatigue test, specimens for rib-to-plate welded joints with partial penetration rates of 65%, 75%, 85%, and double-sided welds were utilized. The detailed information for the test specimens is provided in Table 4.

3.3 Characteristics of the fatigue cracks

Under the influence of the fatigue loading device described above, when the weld penetration rate is 65%, all cracks initiate from the weld root and propagate along the weld throat until the entire throat is penetrated, as illustrated in Figure 9a. For weld penetration rates of 75% or 85%, the majority of fatigue cracks still commence from the weld root and propagate along the

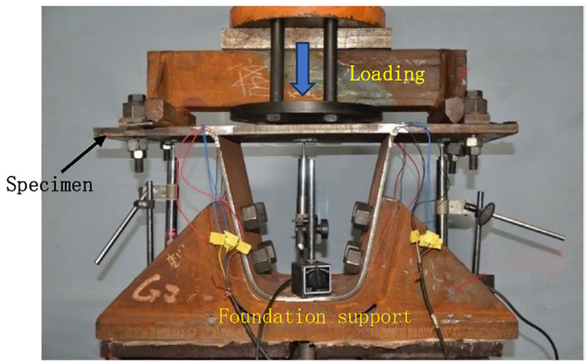

Figure 8. Test loading device. **Source(s):** Authors' own work

Table 4. Information of specimens

Specimens	Welding method	Penetration rate	Amounts of specimens	Loading frequency (Hz)	Loading amplitude (kN)
SP1	Single-side fillet welds	65%	6	3.5–5.0	18–52
SP2	Single-side fillet welds	75%	6	3.5–4.5	30–52
SP3	Single-side fillet welds	85%	6	3.0–4.5	40–55
SP4	Double-side fillet welds	Double-side	8	3.5–4.0	48–61

Source(s): Authors' own work

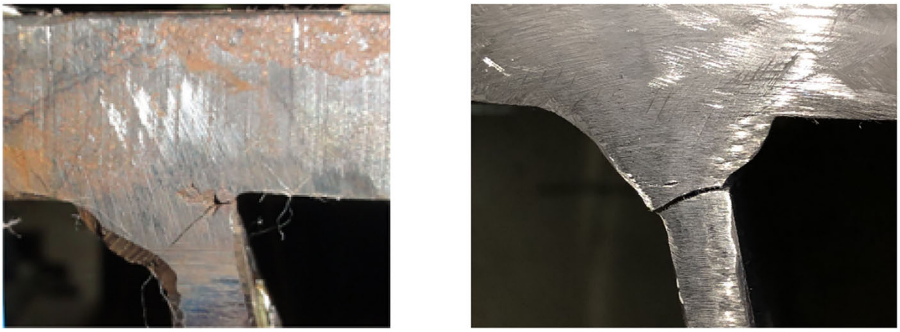

Weld penetration rate of 65%
(a)

Double-side welding
(b)

Figure 9. Cross-section of a cracking joint. **Source(s):** Authors' own work

weld throat. However, 3 cracks initiate from the weld toe on the inner side of U-shaped ribs and develop along the rib web until the U-shaped rib web is penetrated. In double-side welded joints, the cracks predominantly start from the inner side of the U-shaped rib weld and develop along the U-shaped rib web, as depicted in Figure 9b.

3.4 Fatigue S-N curves

The nominal stress of the U-shaped rib-to-deck welded joint in OSDs can be determined based on the normal stress amplitude caused by the bending in the U-shaped rib. A simplified model of the test loading specimen was established using Midas Civil. The bottoms of the U-shaped rib were completely fixed. The bending moment distribution is depicted in Figure 10. The nominal stress is determined based on the bending moment distribution and the actual load applied to each specimen.

According to Eurocode 3 specifications, the fatigue strength of this structural detail is 71 MPa, and its S-N curve is depicted in Figure 11. Notably, the test data are predominantly situated above the curve. Despite the evident dispersion in the test data, a clear observation emerges: the fatigue performance of double-side welded joints surpasses that of partial penetration welded joints. Under the same nominal stress, double-side welded joints exhibit significantly higher loading cycles compared to partial penetration welded joints.

S-N fatigue curve regression was performed on the test data for the partial penetration weld and the double-sided weld, respectively.

Firstly, the loading cycles and nominal stress range for partial penetration welded specimens are shown in the graph with double logarithmic coordinates. Through regression

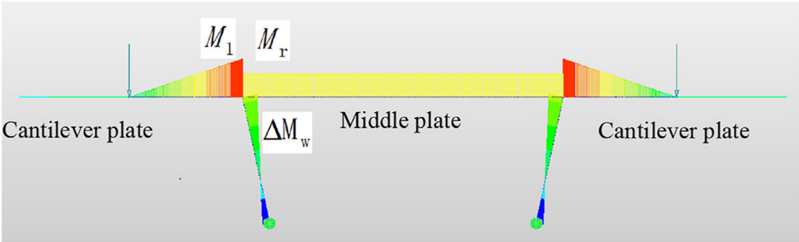

Figure 10. Bending moment distribution. **Source(s):** Authors' own work

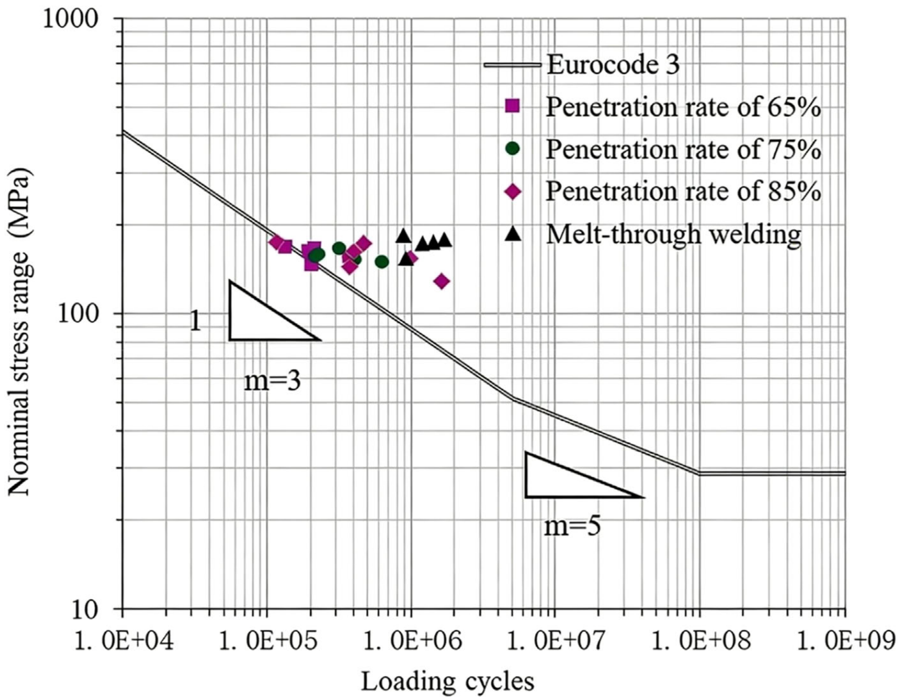

Figure 11. Relationship between nominal stress and loading cycles. **Source(s):** Authors' own work

analysis, the regression equation of the S-N fatigue curve can be obtained as shown in Equation (1):

$$\mathrm{lgN} = 18.1576 - 5.7457\,\mathrm{lg}\,\Delta\sigma \tag{1}$$

When $N = 2{,}000{,}000$, the nominal stress range $\Delta\sigma = 115.7\,\mathrm{MPa}$.

In this case, the correlation coefficient $r = -0.6772$, and the mean squared deviation $s = 0.2221$. Subtract the standard deviation of 2 times lgN from the above formula and take the 97.7% guarantee rate. The regression equation is shown in Equation (2):

$$\mathrm{lgN} = 17.7129 - 5.7457\,\mathrm{lg}\,\Delta\sigma \tag{2}$$

When N = 2,000,000, the nominal stress range $\Delta\sigma = 96.9$ MPa.

Then, the loading cycles and nominal stress range for double-side welded specimens are shown in the graph with double logarithmic coordinates. Through regression analysis, the regression equation of the S-N fatigue curve can be obtained as shown in Equation (3):

$$\mathrm{lgN} = 17.1063 - 4.8904\,\mathrm{lg}\,\Delta\sigma \tag{3}$$

When N = 2,000,000, the nominal stress range $\Delta\sigma = 162.0$ MPa.

In this case, the correlation coefficient $r = -0.5192$, and the mean squared deviation $s = 0.126$. Subtract the standard deviation of 2 times lgN from the above formula and take the 97.7% guarantee rate. The regression equation is shown in Equation (4):

$$\mathrm{lgN} = 16.8543 - 4.8904\,\mathrm{lg}\,\Delta\sigma \tag{4}$$

When N = 2,000,000, the nominal stress range $\Delta\sigma = 143.9$ MPa.

From the above calculation results, it can be found that the fatigue strength of double-side welded joint is higher than that of partial penetration welded joint, therefore, on the premise that the double-side welding construction quality can be guaranteed, double-side weld should be advocated to use on U-shaped rib-to-deck welded joint in OSDs.

4. Conclusion

The main conclusions of this study are summarized as follows:

(1) The finite element model of U-shaped rib-to-deck welded joints, incorporating penetration rates of 65%, 75%, 85%, and double-sided welds, was established. Mechanical characteristics under typical loading conditions were analyzed. Increasing the penetration rate of partial penetration welds resulted in a weakening of stress concentration at the welding root. In comparison, double-side welding, by eliminating the welding root, reduced the degree of stress concentration.

(2) Penetration depth testing of partial penetration specimens, conducted using phased array ultrasonic testing technology, revealed a significant dispersion in penetration depth. Even within the same weld with a length of 300 mm, variations in penetration depth were observed. The actual penetration rates for design penetration rates of 65%, 75%, and 85% are 72.2%, 77.6%, and 85.9%, respectively.

(3) Fatigue test results indicated that fatigue cracks in double-side welded joints initiated at the inner welding toe of the U-shaped ribs and propagated along the thickness direction of the U-shaped rib web. In contrast, fatigue cracks in partial penetration welded joints primarily started at the welding root of the unfused weld and developed along the welding throat until penetrating the entire welding throat.

(4) Fatigue S-N curves were regressed for both partial penetration and double-side welded joints. The fatigue S-N curve for partial penetration welded joints is represented by lgN = 17.7129–5.7457 lgσ, with a corresponding fatigue strength of 96.9 MPa when N = 2,000,000. For double-side welded joints, the fatigue S-N curve is lgN = 16.8543–4.8904 lgσ, with a corresponding fatigue strength of 143.9 MPa when N = 2,000,000. Notably, the fatigue performance of double-sided welds was found to be superior to that of partial penetration welds.

References

American Association of State Highway and Transportation Officials. (2012). *AASHTO LRFD bridge design specifications* (6th ed.). Washington, DC: American Association of State Highway and Transportation Officials (AASHTO).

Chen, J., Wei, C., & Zhao, Y. (2023). Fatigue resistance of orthotropic steel deck system with double-side welded rib-to-deck joint. *Advances in Structural Engineering*, *26*(5), 952–965. doi: 10.1177/13694332221146858.

Chen, F., Liu, Q., Lu, Y., Luo, Y., Xiao, X., Liu, Y., . . . Chen, Y. (2024). Fatigue reliability assessment of rib-to-deck double-sided welded joints in orthotropic steel decks considering welding residual stress. *Scientific Reports*, *14*(1), 31418. doi: 10.1038/s41598-024-83091-2.

China Railway Corporation. (2017). *Code for design of railway earth structure (TB 10091-2017)*. Beijing: China Railway Publishing House.

Cui, C., Bu, Y. Z., & Zhang, Q. H. (2015). Fatigue property assessment methods for weld joint in orthotropic steel bridge deck. *China Journal of Highway and Transport*, *28*(7), 52–57, 76.

Cui, C., Zhang, Q., Luo, Y., Hao, H., & Li, J. (2018). Fatigue reliability evaluation of deck-to-rib welded joints in OSD considering stochastic traffic load and welding residual stress. *International Journal of Fatigue*, *111*, 151–160. doi: 10.1016/j.ijfatigue.2018.02.021.

Eurocode 3 (2005). *Design of steel structures. EN 1993-1-1: General rules and rules for buildings*: European Commission.

Japan Road Association. (2002). *Fatigue design guidelines for steel highway bridges*. Tokyo: Japan Road Association (JRA).

Ju, X., & Tateishi, K. (2014). Fatigue crack behavior at rib-to-deck weld bead in orthotropic steel deck. *Advances in Structural Engineering*, *17*(10), 1459–1468. doi: 10.1260/1369-4332.17.10.1459.

Li, M., Cui, C., Wang, H., Zhang, Q., Da, L., & Bu, Y. (2023). Fatigue behavior and remaining life evaluation of rib-to-deck joints using interior repair welds. *Thin-Walled Structures*, *183*, 110378. doi: 10.1016/j.tws.2022.110378.

Li, X., Lin, H., Zhao, A., Wang, R., Feng, Z., Zhang, S., . . . Xu, X. (2024). Experimental study on fatigue performance of double welded orthotropic steel bridge deck. *Journal of Constructional Steel Research*, *213*, 108418. doi: 10.1016/j.jcsr.2023.108418.

Ministry of Transport of the People's Republic of China (2015). *Specifications for design of highway subgrades (JTG D64-2015)*. Beijing, China: China Communications Press.

National Railway Administration of the People's Republic of China (2017). *Code for design on steel structure of Railway bridge (TB 10091-2017)*. Beijing: China Railway Publishing House. 2017.

Pu, Q., Gao, L., Liu, Z., & Shi, Z. (2013). Fatigue assessment of orthotropic steel bridge deck based on hot spot stress method. *Journal of Southwest Jiaotong University*, *48*(3), 395–401.

Sim, H. B., & Uang, C. M. (2012). Stress analyses and parametric study on full-scale fatigue tests of rib-to-deck welded joints in steel orthotropic decks. *Journal of Bridge Engineering*, *17*(5), 765–773. doi: 10.1061/(asce)be.1943-5592.0000307.

Sim, H. B., Uang, C. M., & Sikorsky, C. (2009). Effects of fabrication procedures on fatigue resistance of welded joints in steel orthotropic decks. *Journal of Bridge Engineering*, *14*(5), 366–373. doi: 10.1061/(asce)1084-0702(2009)14:5(366).

Tao, X. (2013). Experimental study on the fatigue performance of the section model of orthotropic steel bridge deck. *China Railway Science*, *34*(4), 22–26.

Tong, L., Wang, T., Yu, Q., Zhao, X. L., & Xu, X. (2023). Experimental study on fatigue behavior of trapezoidal rib-to-deck welded joints in orthotropic steel decks strengthened with CFRP sheets. *Advances in Structural Engineering*, *26*(6), 1130–1141. doi: 10.1177/13694332231153968.

Wang, D., Dong, Y., Pan, Y., & Ma, R. (2020). Machine vision-based monitoring methodology for the fatigue cracks in U-rib-to-deck weld seams. *IEEE Access*, *8*, 94204–94219. doi: 10.1109/access.2020.2995276.

Wang, Q., Fu, Z., Wei, Y., & Wang, Y. (2023). Fatigue evaluation of the rib-deck weld in OSDs considering the effect of asphalt-steel interface bonding property. *Advances in Structural Engineering*, *26*(8), 1486–1497. doi: 10.1177/13694332231165347.

Wei, X., & Jiang, S. (2017). Fatigue life prediction on rib-to-deck welded joints of steel bridge deck based on LEFM. *Journal of Southwest Jiaotong University*, *52*(1), 16–22.

Xiao, Z. G., Yamada, K., Ya, S., & Zhao, X. L. (2008). Stress analyses and fatigue evaluation of rib-to-deck joints in steel orthotropic decks. *International Journal of Fatigue*, *30*(8), 1387–1397. doi: 10.1016/j.ijfatigue.2007.10.008.

Ya, S., Yamada, K., & Ishikawa, T. (2011). Fatigue evaluation of rib-to-deck welded joints of orthotropic steel bridge deck. *Journal of Bridge Engineering*, *16*(4), 492–499. doi: 10.1061/(asce)be.1943-5592.0000181.

Corresponding author
Xiaochen Ju can be contacted at: juxc2008@163.com

Xiaochen Ju is a Research Fellow from China Academy of Railway Sciences Corporation Limited. Specialized in Bridge Engineering, his research focuses on fatigue performance, structural stability and operation & maintenance of railway bridges. He has been awarded 7 provincial/ministerial-level scientific research prizes, obtained 8 invention patents, and published more than 20 papers indexed by SCI and EI.